Simulation and Experimental Results of Irradiated Power Diodes

R. Siemieniec[*], D. Schipanski[*], W.Südkamp[**], J.Lutz[***]
[*]Technical University of Ilmenau, PO Box 100565, D - 98684 Ilmenau
[**]Technical University of Berlin, Jebensstraße 1, D - 10623 Berlin
[***]Semikron Elektronik GmbH, Sigmundstraße 200, D - 90431 Nürnberg

Acknowledgements

The authors wishes to thank the scientists, especially Dr. Nürnberg and Prof. Gajewski from the Weierstrass Institute for Applied Analysis and Stochastics in Berlin, who developed the device simulator ToSCA. In addition the authors are grateful for their support and the addition of new features and algorithms into the simulation system.
This work is supported by grants of the Deutsche Forschungsgemeinschaft.

Keywords

Power Semiconductor Devices, Simulation, Measurements

Abstract

An advanced recombination model based on the Shockley-Read-Hall-statistics with full trap dynamics is used for the simulation of irradiated power diodes. The model makes use of the rate equations which also take into account the dynamic effects in the space charge region of the power devices. The high-level lifetime calculated from DLTS (Deep Level Transient Spectroscopy) data does not agree well with the lifetime determined by lifetime measurements. An agreement is achieved by means of a temperature dependent capture coefficient of the dominating recombination center E(90K), calculated from the lifetime measurement results. Simulations and measurements are done to determine the dependencies of reverse recovery current maximum and reverse recovery charge on temperature. By use of the calculated capture coefficient, a sufficient agreement between simulation and measurement is achieved.

1 Introduction

Lifetime killing is usually used for optimization of the power device characteristics. By applying irradiation (e.g. with electrons, with protons or with alpha particles), it is possible to generate homogenous or local lifetime profiles. With specific profiles, a better device characteristic can be achieved compared to the well-known recombination centers gold and platinum [1].
Irradiation generates centers with different energy levels in the band gap of Silicon semiconductors. It was shown that donor-states of radiation-induced traps change the dynamic electrical properties in a semiconductor device [2]. Furthermore, the temperature dependence of device parameters is different when irradiation-induced centers are used instead of platinum or gold [3].
Previous simulation tools cannot predict this behavior because they only use a stationary lifetime model and take into account only one recombination center level. Since irradiation generates more than one recombination center, and high-level, low-level and generation lifetime are controlled by different centers (Appendix A), the use of an extended recombination model becomes necessary. In this work we present a new device simulation with full trap dynamics using the device simulator ToSCA [4] and compare the simulations with measurements on different irradiated power diodes.

2 Recombination model

Common device simulation tools offer a simple recombination model as default choice using the well known Shockley-Read-Hall equation (eq.1). This model describes the recombination process which occurs through trapping mechanisms [5],[6]. For a trap or recombination center it is assumed that it

has an energy level in the band gap and its charge state may have one of two values differing by one electronic charge:

$$R_{SRH} = \frac{pn - n_i^2}{\tau_{p0}(n + n_1) + \tau_{n0}(p + p_1)} \quad (1)$$

Here the electron and hole concentrations are given by n and p, their product under equilibrium conditions being n_i^2. The minority carrier lifetimes for electrons and holes are determined by τ_{n0} and τ_{p0}, while the terms n_1 and p_1 describe the energy level where the recombination centers are found.
But this simple model does not include more than one recombination center as well as the trap charging processes which strongly influence the dynamic behavior of the power device. Therefore the device simulator ToSCA uses a new implemented model including full trap dynamics of independent recombination centers with two charge states, avoiding these problems (Appendix B).

3 Manufactured Samples

Samples were prepared using the Semikron CAL-diode (CAL: Controlled Axial Lifetime) production line. All devices have an active area of 6mm^2 and were annealed at over 300°C for one hour. In order to perform DLTS measurements, the junction depth is varied as shown in Table I. Sample EH contains the most important lifetime adjustment steps of the CAL-Diode. In Sample H, the He^{2+}-dose was reduced to 10% of sample EH to allow the evaluation of the electric parameters of the recombination centers. The rated current is about 10A (166A/cm^2), the rated voltage is 1200V.

Table I - Sample overview

Type	Irradiation	Dose	pn-junction depth	Base width
EH	Electron Helium	100% 100%	22µm	85µm
N	none	-	11.5µm	95µm
E	Electron	100%	22µm	85µm
H	Helium	10%	11.5µm	95µm

4 Measurement Techniques

4.1 DLTS Measurements

With Deep Level Transient Spectroscopy (DLTS), pulsed base capacitance transients of a pn-junction with deep levels are analyzed as a function of temperature [7]. During a fill-pulse, deep levels like recombination centers are filled with charged carriers and during the reverse phase, the deep levels are discharged by thermal emission, creating an exponential capacitance transient. The time constant of the transient decreases with temperature with the arrhenius factor $\exp(E_T/k_BT)$. The transient is sampled at two time points t_1, t_2 and the difference - the DLTS signal - is recorded as a function of temperature. If the rate window $(t_2-t_1)/\ln(t_2/t_1)$ corresponds to the emission time constant, the DLTS signal reaches a maximum. The intensity of the DLTS peaks are proportional to the trap density. To obtain the most important trap parameters energy level and the range of capture cross section, an arrhenius plot can be constructed by variation of the rate window for a trap. However, in most cases the capture cross section must be measured directly by variation of the fill-pulse duration because of the entropy factor and temperature dependence of the capture cross section.

4.2 OCVD Measurements

The concept of the Open Circuit Voltage Decay (OCVD) method was introduced in 1955 [8]. Nowadays, it is a valid method and has found widespread acceptance. Using OCVD measurement, a steady-state excess carrier concentration is applied by a forward current flow through a diode (fig.1a). After an abrupt opening of the circuit at t=0, recombination of excess carriers will take place and the diode's open voltage is monitored (fig.1b). The initial voltage step at t=0 is due to the ohmic voltage

drop V_0 in the diode, which is observed when the current flow stops. This voltage drop may be used to determine of the device's series resistance. The strong drop in the V-t-curve near t=0 is caused by emitter recombination. This effect becomes negligible for $t > 2.5\tau_b$, where τ_b is the base lifetime. It is possible to estimate the lifetime from the linear slope.

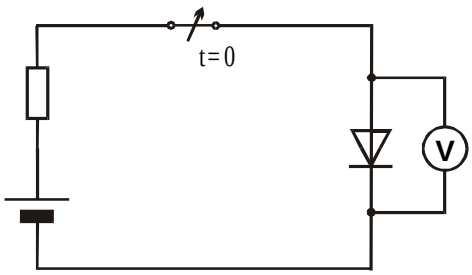

Fig.1a: OCVD schematic

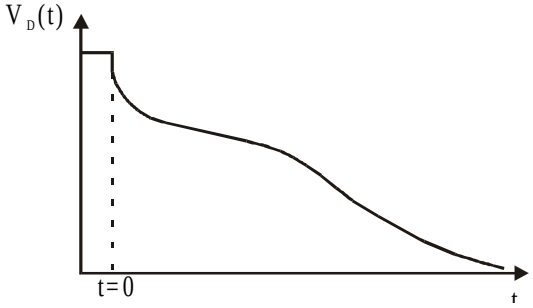

Fig. 1b: OCVD voltage waveform

For diodes with a pin-structure as used in these investigations, the lifetime under high injection condition (high-level lifetime) is given by the equation:

$$\tau_{HL} = \frac{2k_B T}{e}\left(\frac{dV}{dt}\right)^{-1} \tag{2}$$

To check if the device is in the high injection mode, the carrier concentration is calculated by using eq.3. High injection is found if p becomes large compared to the base doping ($p > 100\ N_D$).

$$p = n_i \cdot \exp\left(\frac{V_0}{\frac{2k_B T}{e}}\right) \tag{3}$$

4.3 Reverse Recovery Measurements

The reverse recovery (RR) measurement is one of the standard electrical lifetime characterization techniques. For the determination of carrier lifetimes, different methods using charge storage analysis are employed [9], [10]. At high excess charges, the lifetime is found to be too small [11]. For that reason, reverse recovery measurements were only used for the characterization of the device's turn-off behavior. Fig.2 shows the circuit diagram for the reverse recovery measurements.

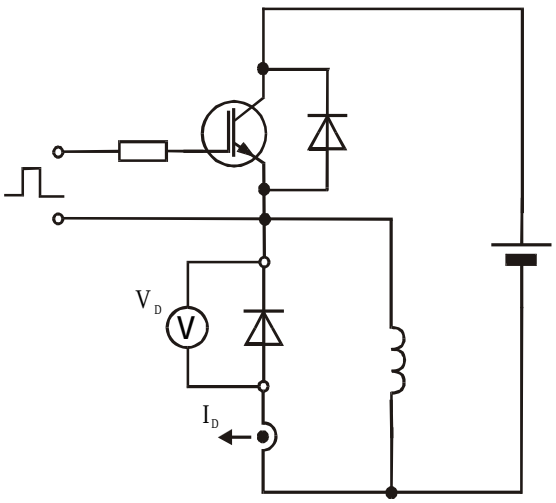

Fig. 2: Circuit diagram for reverse-recovery measurements

5 Recombination center parameters

5.1 DLTS results

5.1.1 Recombination center data

The recombination center parameters necessary to perform simulations were determined by DLTS measurements. Due to limitations of the DLTS measurement technique, several parameters must be determined by additional measurements. For example the capture coefficient c_p of the trap E(230K) is determined by leakage current measurements since E(230K) controls the generation lifetime. The ratio of the capture coefficients c_p/c_n of the trap E(90K) is calculated from the attenuation of the DLTS signal during minority carrier injection. Table II gives an overview of the traps found in the irradiated devices. They are in good agreement with the literature [2],[13],[14].

Table II - DLTS results

Trap	Energy level	Capture Coefficient		Entropy factor	
		c_n [cm^3/s]	c_p [cm^3/s]	χ_n	χ_p
E(90K): A-Center	E_C-E_T=0.164eV	$2.4*10^{-7}$	$4.8*10^{-6}$	0.25	4
E(230K): Multivacancy	E_C-E_T=0.447eV	$8.09*10^{-8}$	$1.08*10^{-7}$	0.88	1.14
H(195K): K-Center	E_T-E_V=0.353eV	$4.14*10^{-10}$	$2.92*10^{-9}$	0.3	3.44

5.1.2 Recombination center profiles

DLTS measurement is also used for the determination of the concentration profiles. For the electron irradiated sample E, a homogenous profile is found for E(90K) and H(195K), E(230K) was not detectable:

$$N_{E(90K)} = 3.27*10^{13}cm^{-3}$$
$$N_{H(195K)} = 5.51*10^{13}cm^{-3}$$

The Helium irradiation of Sample H leads to inhomogeneous local concentration profiles of the different traps as shown in fig.3. Because of the high trap concentration, only the concentration profile of the minority carrier DLTS signal H(195K) could be determined by first using an injection pulse in forward direction which fills the hole traps. Then a clear pulse discharges the traps in a fraction of the space charge region, which depends on the reverse voltage of this clear pulse.

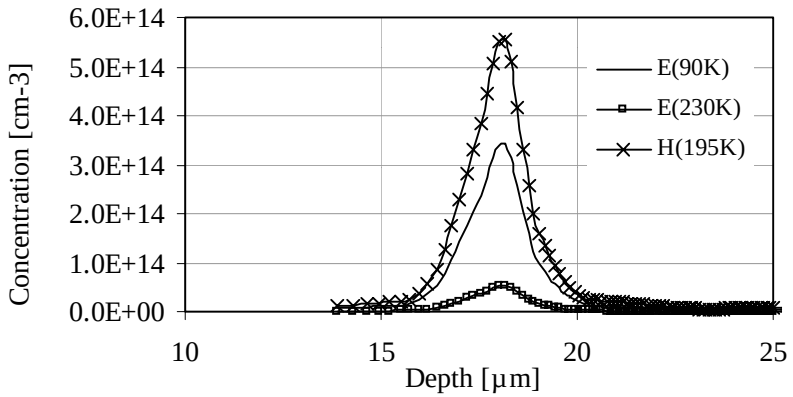

Fig. 3: Trap concentration profiles of the He^{2+}-irradiated sample H

Simulations of the electron occupation after the clear pulse show a resolution of the profile measurement in the range of 1µm. Hence a broader peak is found. For this reason, the sample was further annealed, which causes a reduction of the trap concentrations and an increase of the OCVD lifetime. The OCVD lifetime leads to an average lifetime depending on the recombination center

maximum [12]. After annealing, the concentration profile of E(230K) was determined. The OCVD lifetime and DLTS signal data show that the E(230K) concentration maximum of the annealed sample H was about one fifth of the non annealed sample H. For H(195K) and E(90K) the same profile is assumed and the maximal concentrations are approximated from the amplitude of the DLTS signal in relation to the DLTS signal of E(230K).

5.2 OCVD measurements and high-injection lifetimes

OCVD measurements are performed to determine the effective lifetime in the low-doped n-region. This lifetime represents a high-level lifetime (eq.2). For devices with a homogenous lifetime this is used to estimate the minority carrier lifetimes τ_{n0} and τ_{p0} which are part of the basic parameter set in device simulation.
The high-level lifetime of the electron irradiated sample E is controlled by the electron capture coefficient c_n of the trap E(90K):

$$\tau_{HL} = \tau_{n0} + \tau_{p0} = \frac{1}{c_n \cdot N_T} + \frac{1}{c_p \cdot N_T} \approx \frac{1}{c_n \cdot N_T} \qquad (4)$$

Table III contains the OCVD lifetimes as well as the calculated DLTS lifetimes (for samples N and E). The comparison of the lifetime of sample E as estimated from OCVD and the one from DLTS data show a notable discrepancy. This deviation is because the DLTS data of the capture coefficients measured at low temperatures (80...100K) were found to be nearly temperature independent and were extrapolated to room temperature, whereas the OCVD lifetime is measured at temperatures of 300 and 400K. In this temperature range, the capture coefficient clearly depends on temperature, as shown in table III. A similar behavior is observed in [15]. Thus, for simulations the electron capture rate of E(90K) is estimated according to eq.4, which leads to:

E(90K): $c_n(300K)=3.73*10^{-8}\,cm^3/s$ $c_n(400K)=3.06*10^{-8}\,cm^3/s$

Table III - Sample lifetimes

Type	Lifetime [µs]		
	DLTS	OCVD (300K)	OCVD (400K)
N	> 18	22.7	28
E	0.13	0.82	1.0

6 Reverse Recovery measurements and comparison to simulations

6.1 Comparison of measured and simulated waveforms

It is not possible to measure the concentration profile of sample EH, since the local peak of the Helium irradiation is now located in the p-region of the diode. For the simulation of sample EH, the profile of sample H as shown in fig.3 is multiplied by 10 due to the higher irradiation dose. Nevertheless, emitter recombination effects may now play a more significant role than in sample H, where the recombination center peak is located in the low-doped n-region. The defects generated by the electron irradiation are taken into account just as for sample E. Figures 4-7 show the measured and simulated reverse recovery slopes of the examined samples for a forward current of 10A at a temperature of 400K. The battery voltage is 250V, the di/dt of approximately 500A/µs is adjusted by the gate resistor of the IGBT (fig.2).
The different voltage slopes in simulation and measurement are caused by an insufficient fitting of the IGBT simulation parameters.

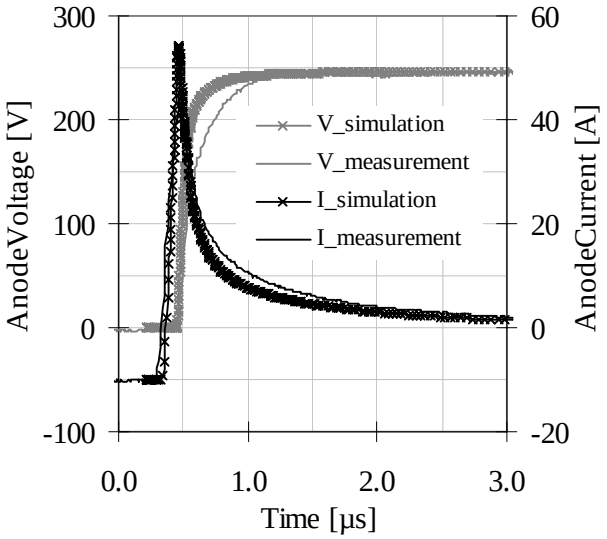

Fig. 4: Reverse recovery of sample N

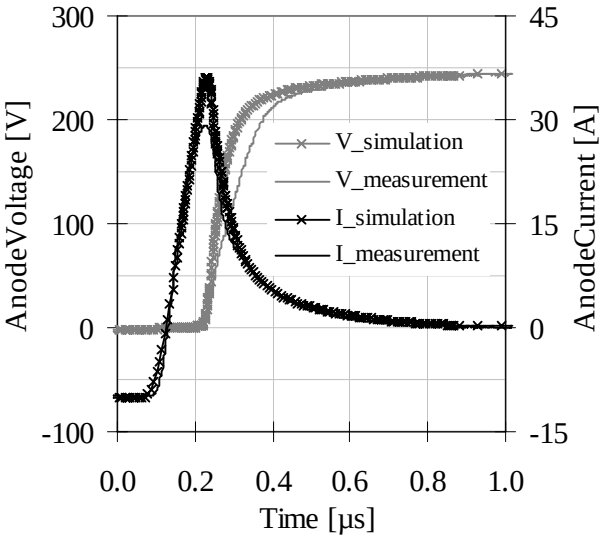

Fig. 5: Reverse recovery of sample E

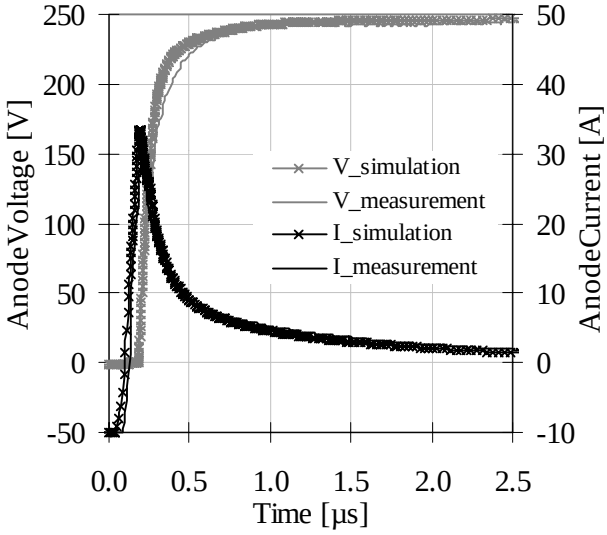

Fig. 6: Reverse recovery of sample H

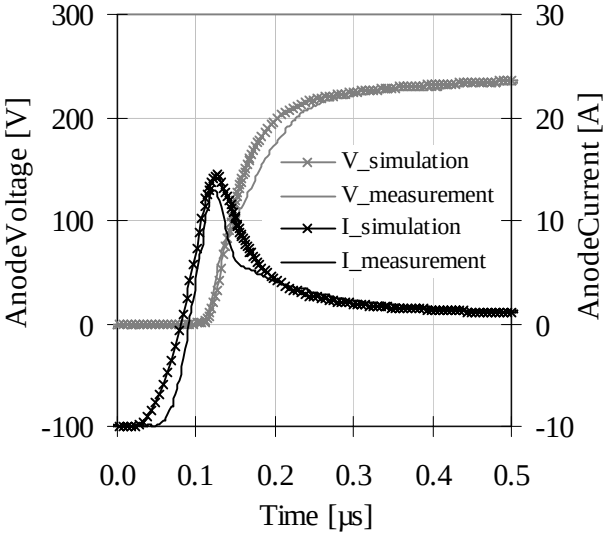

Fig. 7: Reverse recovery of sample EH

6.2 Reverse Recovery Current Maximum

Figures 8-11 show the comparison of simulation and measurement of the reverse recovery current maximum I_{RRM} as a function of the rate of current increase di/dt at a battery voltage of 250V.

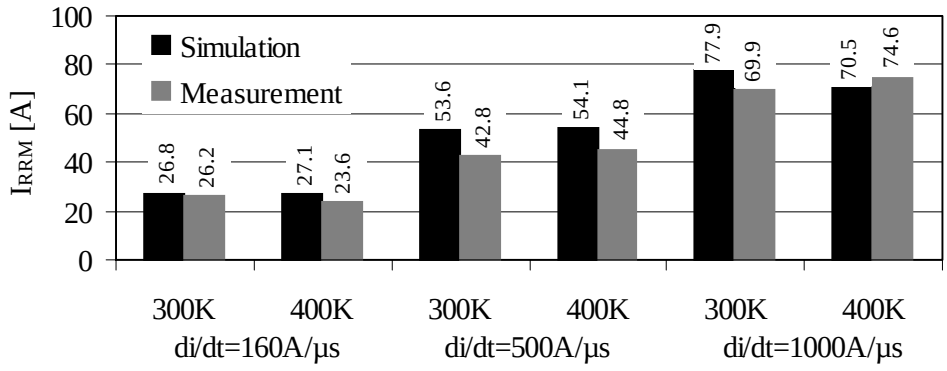

Fig. 8: I_{RRM} versus di/dt for sample N

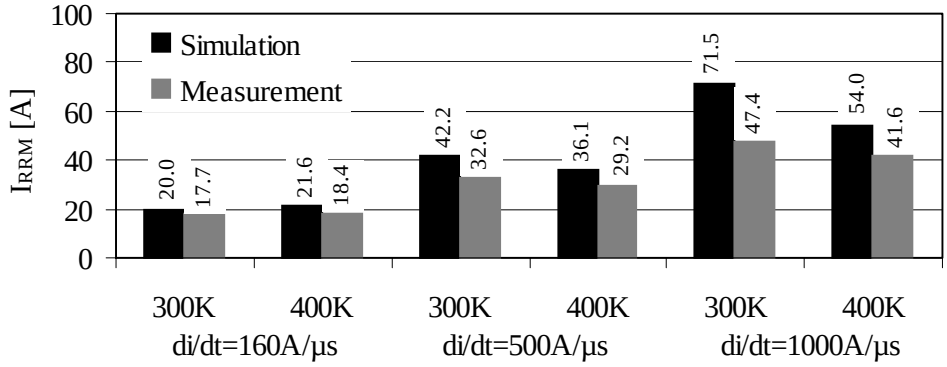

Fig. 9: I_{RRM} versus di/dt for sample E

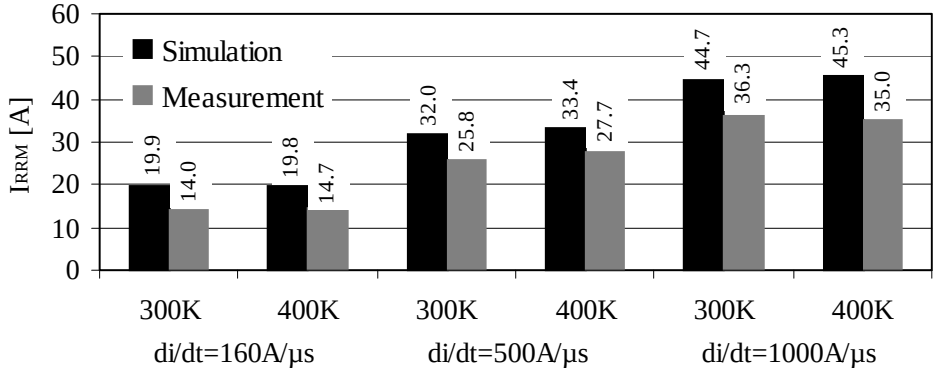

Fig. 10: I_{RRM} versus di/dt for sample H

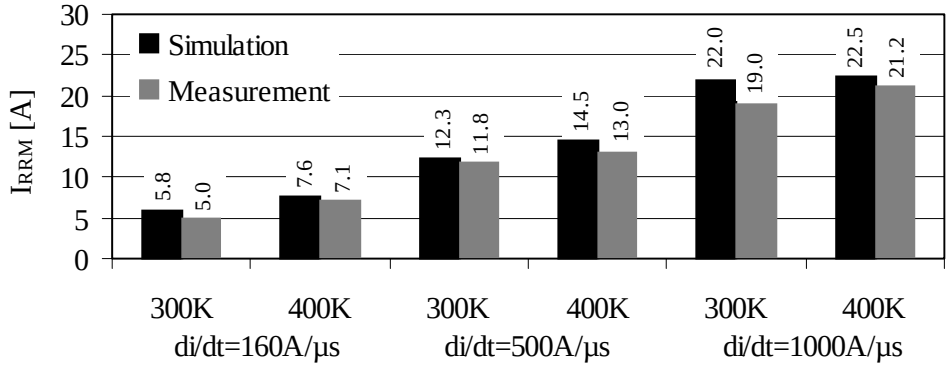

Fig. 11: I_{RRM} versus di/dt for sample EH

A sufficient agreement between the simulated recovery current maximum I_{RRM} of the different samples and the measurements is observed. The I_{RRM} of sample E shows the greatest difference between simulation and measurement at a temperature of 300K. The lifetime, measured by OCVD, is probably too high. In measurements and simulations of I_{RRM}, a weak temperature dependence in the range of 300K to 400K is observed. Generally, the simulation allows the characterization of the device behavior in good agreement with measurements on manufactured samples with different irradiation.

6.3 Reverse Recovery charge

Fig. 12 shows the comparison of measured and simulated data for reverse recovery charge Q_{RR} at a battery voltage of 250V and a forward current of 10A. Varying di/dt in the range of 160A/µs to 1000A/µs shows no influence on reverse recovery charge. The simulated Q_{RR} at 400K is in better agreement with the measurement than at 300K. Again, the lifetime, measured by OCVD, might be too high as shown in the last chapter. However, considering the very different samples and the wide spread of measurement conditions, simulations and measurements show sufficient agreement.

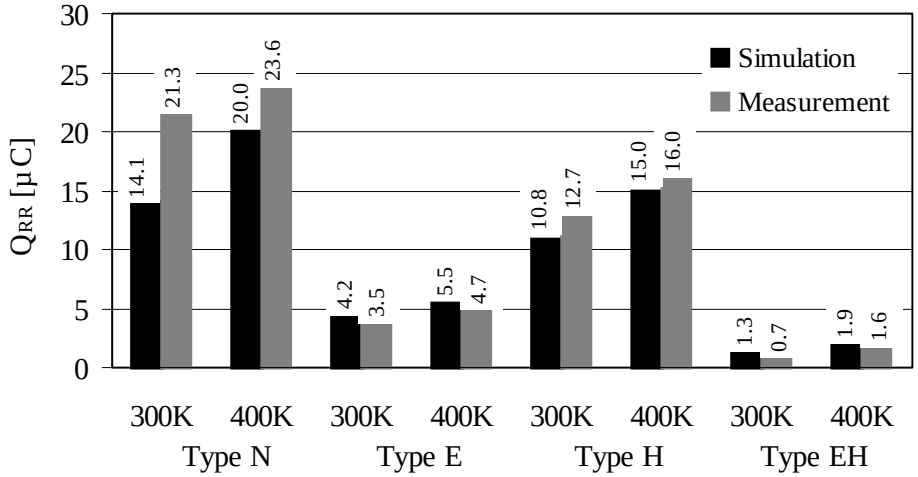

Fig. 12: Comparison of Reverse Recovery Charge

7 Conclusion

The use of an extended recombination model including full trap dynamics results in a satisfactory simulation of irradiated devices. This advanced model also considers charging processes of the recombination centers, which allows a correct transient simulation of the space charge region. Moreover, the introduction of more than one recombination center with different recombination properties into simulation allows the correct description of recombination processes under different conditions, such as high- or low-injection or carrier generation in a space charge region, since they are controlled by different centers.

It is not possible to extrapolate the capture coefficient data from DLTS measurements at low temperatures to the device's working temperature range. Based on the determination of the effective high-level lifetime by OCVD measurements, one can estimate the electron capture coefficient of the trap E(90K) at operating temperature. This is possible because E(90K) controls the high-level lifetime. Introducing those parameters into the simulations, a sufficient agreement between experiment and simulation under different conditions such as various current ratings and temperatures can be achieved.

Nevertheless, more work has to be done on the determination of simulation parameters of both IGBTs and Diodes, in order to allow more exact simulations. The determination of the necessary parameters for the induced recombination centers is still a significant problem, especially the determination of the trap concentration profile at high trap concentrations. There is also the necessity for an investigation of the temperature dependence of the capture cross section in a larger temperature interval than it is possible by DLTS measurements. Furthermore, uncertainties in the effective lifetime determination by OCVD measurements have to be overcome, for instance by the use of optical lifetime determination techniques.

References

1. J.Lutz. *Axial Recombination Center Technology for Freewheeling Diodes*, Proceedings of the 7th EPE, Trondheim, (1997)
2. J.Lutz, W.Südkamp and W.Gerlach. *Impatt Oscillations in Fast Recovery Diodes due to Temporarily Charged Radiation-Induced Deep Levels,* Solid State Electronics Vol. 42, No 6, pp 931-938 (1998)
3. J.Lutz, U.Scheuermann. *Advantages of the New Controlled Axial Lifetime Diode*, Proceedings of the 28th PCIM (1994)
4. Gajewski et al. *ToSCA-Handbuch*, WIAS Berlin, 1994
5. W.Shockley, W.T.Read. *Statistics of the recombinations of holes and electrons*, Physical Review, Vol.87, No.5, pp.835-842, September 1952

6. R.N.Hall. *Electron-Hole Recombination in Germanium*, Physical Review, Vol.87, No.2, p387, Juky 1952
7. D.V.Lang. *Deep-level transient spectroscopy: A new method to characterize traps in semiconductors*, Journal of Applied Physics, Vol.45, No.7, pp.3023-3032, July 1974
8. S.R.Lederhandler, L.J.Giacoletto. *Measurement of Minority Carrier Lifetime and Surface Effects in Junction Devices*, Proc. IRE, pp.477-483, April 1955
9. D.K.Schroder. *Semiconductor Material and Device Characterization*, pp.394-398, Jon Wiley and sons, 1990
10. H.Schlangenotto, W.Gerlach. Solid-State Electronics, Vol. 12, p.267, 1969
11. H.Schlangenotto, W.Gerlach. *On the Post-Injection Voltage Decay of p-s-n Rectifiers at High Injection Level*, Solid-State Electronics, Vol. 15, pp.393-402, 1972
12. J.Vobecky, P.Hazdra, V.Zahlava. *OCVD Lifetime of Ion Irradiated P-i-N Diodes*, Proceedings of the ISPS'98, pp.47-52, Praha, 1998
13. W.Wondrak. *Erzeugung von Strahlenschäden in Silizium durch hochenergetische Elektronen und Protonen*, Dissertation, Universität Frankfurt am Main, 1985
14. A.Hallen, N.Keskitalo, F.Masszi, V.Nagl. *Lifetime in proton irradiated silicon*, Journal of Applied Physics 79 (08), pp.3906, April 1996
15. H.Bleichner, P.Jonsson, N.Keskitalo, E.Nordlander. *Temperature and injection dependence of the Shockley-Read-Hall Lifetime in electron irradiated n-type silicon*, Journal of Applied Physics 79 (12), pp.9142, June 1996

Appendix A - High-level-, Low-level- and generation lifetime for a single recombination center

A - Shockley-Read-Hall-Recombination rate and lifetime

From eq.1 and with $n=n_0+\delta p$ one obtains:

$$R = \frac{\delta n\, p_0 + \delta p\, n_0 + \delta n\, \delta p}{\tau_{p0}\left[n_0 + \delta n + N_C \exp\left(\frac{E_T - E_C}{k_B T}\right)\right] + \tau_{n0}\left[p_0 + \delta p + N_V \exp\left(\frac{E_V - E_T}{k_B T}\right)\right]}$$

$$\delta n = \delta p$$

$$\tau = \frac{\delta n}{R} = \tau_{p0}\left[\frac{n_0 + \delta n + N_C \exp\left(\frac{E_T - E_C}{k_B T}\right)}{n_0 + p_0 + \delta n}\right] + \tau_{n0}\left[\frac{p_0 + \delta n + N_V \exp\left(\frac{E_V - E_T}{k_B T}\right)}{n_0 + p_0 + \delta n}\right]$$

$$\tau_{n0} = \frac{1}{c_n \cdot N_T} \qquad \tau_{p0} = \frac{1}{c_p \cdot N_T}$$

B - Low-level lifetime

$n_0 >> \delta n$, $n_0 >> p_0$ (n-type silicon)

$$\tau_{LL} = \tau_{p0}\left[1 + \exp\left(\frac{E_T - E_F}{k_B T}\right)\right] + \tau_{n0} \exp\left[\frac{2E_I - E_T - E_F}{k_B T}\right]$$

C - High-level lifetime

$$\delta n >> n_0, \delta n >> N_C \exp\left(\frac{E_T - E_C}{k_B T}\right)$$

$$\tau_{HL} = \tau_{n0} + \tau_{p0}$$

D - Space Charge Generation (Generation lifetime)

Because the generation current in the space charge region is given by

$$J_G = q\,R\,w_{SCR} = \frac{q\,n_i\,w_{SCR}}{\tau_{SC}}$$

and assuming $n,p<<n_i, n << N_C \exp\left(\frac{E_T - E_C}{k_B T}\right), p << N_V \exp\left(\frac{E_V - E_T}{k_B T}\right)$

one obtains for the generation lifetime

$$\tau_{SC} = \tau_{p0} \exp\left(\frac{E_T - E_I}{k_B T}\right) + \tau_{n0} \exp\left(\frac{E_I - E_T}{k_B T}\right)$$

Appendix B - Trap recombination model equations

A - Poison Equation

$$-\operatorname{div}(\varepsilon \cdot \operatorname{grad}\varphi) = e\left[p - n - N_A^- + N_D^+ + \Sigma\left(N_{TD}^+ - N_{TA}^-\right)\right]$$

B - Continuity Equations of Acceptors (Donors have a similar relation)

$$\frac{\partial n}{\partial t} - \operatorname{div} J_n = G - R + \Sigma\left[e_{nA} N_{TA}^- - c_{nA}\, n \left(N_{TA} - N_{TA}^-\right)\right]$$

$$\frac{\partial p}{\partial t} + \operatorname{div} J_p = G - R + \Sigma\left[e_{pA}\left(N_{TA} - N_{TA}^-\right) - c_{pA}\, p\, N_{TA}^-\right]$$

$$e_{nA} = \chi_{nA} c_{nA}\, n_i \exp\left(\frac{E_{TA} - E_I}{k_B T}\right)$$

$$e_{pA} = \chi_{pA} c_{pA}\, n_i \exp\left(\frac{E_I - E_{TA}}{k_B T}\right)$$

C - Probability of an Occupied State of an Acceptor

$$\frac{df_A}{dt} = \left(c_{nA}\, n + e_{pA}\right)\left(1 - f_A\right) - \left(c_{pA}\, p + e_{nA}\right) f_A \qquad N_{TA}^- = N_{TA} \cdot f_A$$

Thus for each trap the capture rates, the energy level, the entropy factors and the trap density is needed.

p	hole concentration	G	generation rate
n	electron concentration	R	recombination rate
N_A	acceptor density	N_D	donor density
N_C	conduction band state density	N_V	valence band state density
N_{TA}	acceptor trap density	N_{TA}^-	ionized acceptor trap density
N_{TD}^+	ionized donor trap density	E_{TA}	acceptor trap energy level
E_T	trap energy level	f_A	fraction of occupied acceptor traps
n_i	intrinsic density	E_i	intrinsic energy level
n_0	electron equilibrium concentration	p_0	hole equilibrium concentration
δn	electron excess concentration	δp	hole excess concentration
c_n	capture rate for electrons	c_p	capture rate for holes
e_n	emission rate for electrons	e_p	emission rate for holes
χ_n	entropy factor for electrons	χ_p	entropy factor for holes
w_{SCR}	space charge region width	J_G	generation current density
τ_{n0}	electron minority carrier lifetime	τ_{p0}	hole minority carrier lifetime